Co-ordination Chemistry of Dimethylgold(III). Synthesis, Structural[†] Studies, and Fluxional Behaviour of Complexes with Polydentate Ligands

Peter K. Byers, Allan J. Canty,* and Nigel J. Minchin
Chemistry Department, University of Tasmania, Hobart, Tasmania, Australia 7001
Jennifer M. Patrick, Brian W. Skelton, and Allan H. White
Department of Physical and Inorganic Chemistry, University of Western Australia, Nedlands, W.A. 6009

Dimethylgold(III) nitrate forms complexes $[AuMe_2L]NO_3$ with polydentate nitrogen-donor ligands (L) containing *N*-methylimidazol-2-yl (mim) and pyridin-2-yl (py) groups: $(mim)_2CHOH$, $(mim)_3COH$, $(py)(mim)_2COH$, and $(py)_2(mim)COH$. The structures of $[AuMe_2\{(py)(mim)_2COH\}]NO_3$ and $[AuMe_2\{B(pz)_4\}]$, where $[B(pz)_4]^-$ is tetrakis(pyrazol-1-yl)borate, have been determined by single-crystal *X*-ray diffraction at 295 K and refined by least-squares methods to *R* 0.034 and 0.040 for 2 801 and 2 240 independent 'observed' reflections, respectively. The complexes have square-planar geometry for gold, '*cis*-$Me_2Au(mim)_2$' in the $(py)(mim)_2COH$ complex and '*cis*-$Me_2Au(pz)_2$' in the $[B(pz)_4]^-$ complex, with one unco-ordinated pyridine and two unco-ordinated pyrazole rings, respectively. The complexes $[AuMe_2L]NO_3$ [L = $(mim)_3COH$ or $(py)_2(mim)COH$] in CD_3OD, and monoprotonated complexes of poly(pyrazol-1-yl)borate ligands, $[AuMe_2\{HB(pz)_2(Hpz)\}]^+$ and $[AuMe_2\{B(pz)_3(Hpz)\}]^+$, in $(CD_3)_2SO-D_2O$, exhibit complex variable-temperature ^1H n.m.r. spectra consistent with fluxional behaviour involving five-co-ordinate intermediates. In addition, the spectra show that $[AuMe_2\{(py)_2(mim)COH\}]NO_3$ in solution exists as two structural isomers, involving '*cis*-$Me_2Au(py)(mim)$' and '*cis*-$Me_2Au(py)_2$' environments in the ratio *ca.* 5:1. Crystal data: $[AuMe_2\{(py)(mim)_2COH\}]NO_3$, triclinic, space group $P\bar{1}$, $a = 11.393(3)$, $b = 10.859(2)$, $c = 7.927(2)$ Å, $\alpha = 89.16(2)$, $\beta = 74.11(2)$, $\gamma = 89.87(2)°$, and $Z = 2$; $[AuMe_2\{B(pz)_4\}]$, monoclinic, space group $P2_1/c$, $a = 12.645(2)$, $b = 8.343(2)$, $c = 17.310(4)$ Å, $\beta = 99.14(2)°$, and $Z = 4$.

Organogold(III) complexes generally have square-planar geometry for the gold atom, *e.g.* the potential tridentate ligands tris(pyridin-2-yl)methane and tris(pyridin-2-yl)methanol, L = $(py)_3CX$ (X = H or OH), in $[AuMe_2L]NO_3$ are present as bidentate ligands to give *cis*-C_2AuN_2 co-ordination with one unco-ordinated ring.[1] The pyrazole donor tripod ligands $(pz)_3CH$ and $[HB(pz)_3]^-$ also form similar complexes,[1,2] but for the complex $[AuMe_2\{(pz)_3CH\}]NO_3$ there is an additional weak axial Au ··· N interaction of 3.139(7) Å.[1]

It has been proposed that one factor favouring axial co-ordination by $(pz)_3CH$, but not $(py)_3CH$, is that the presence of five-membered pyrazole rings results in a ligand geometry that more readily allows a weak axial interaction.[1] To explore further the weak acceptor properties of the *cis*-C_2AuN_2 kernel we have synthesized cationic complexes $[AuMe_2L]NO_3$ where the ligands L are flexible tripod ligands involving pyridin-2-yl and *N*-methylimidazol-2-yl groups, $(py)_n(mim)_{3-n}COH$ (n = 0, 1, or 2), as these ligands have combinations of five- and six-membered donor rings, and basicities greater than that for $(py)_3CX$ and $(pz)_3CH$.[3-5] A complex of the bidentate ligand $(mim)_2CHOH$ has been included for ^1H n.m.r. comparison. Structural studies of $[AuMe_2\{(py)(mim)_2COH\}]NO_3$ and $[AuMe_2\{B(pz)_4\}]$, variable-temperature ^1H n.m.r. studies of the cations $[AuMe_2L]^+$ [L = $(mim)_3COH$ or $(py)_2(mim)COH$], and complementary n.m.r. studies of protonated poly(pyrazol-1-yl)borate cations $[AuMe_2\{HB(pz)_2(Hpz)\}]^+$ and $[AuMe_2\{B(pz)_3(Hpz)\}]^+$ are also reported.

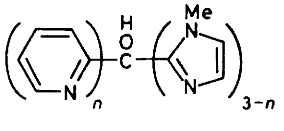
$n = 0$: $(mim)_3COH$
$n = 1$: $(py)(mim)_2COH$
$n = 2$: $(py)_2(mim)COH$

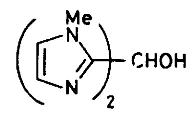
$(mim)_2CHOH$

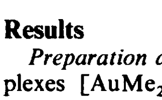
X = H : $(py)_3CH$
X = OH : $(py)_3COH$

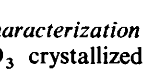
$(pz)_3CH$

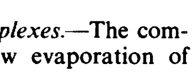
$[HB(pz)_3]^-$

Results

Preparation and Characterization of Complexes.—The complexes $[AuMe_2L]NO_3$ crystallized on slow evaporation of aqueous solutions containing equimolar quantities of dimethyl gold(III) nitrate and ligand. They required purification by recrystallization from methanol, except for the $(py)_2(mim)COH$ complex which was recrystallized from chloroform–ethyl acetate. The complexes form conducting solutions in water and exhibit ^1H n.m.r. spectra indicating the presence of organometal and ligand groups (Table 1).

Solid State Structures of $[AuMe_2\{(py)(mim)_2COH\}]NO_3$ *and* $[AuMe_2\{B(pz)_4\}]$.—Aspects of the molecular geometry of

---

[†] [Bis(*N*-methylimidazol-2-yl)(pyridin-2-yl)methanol]dimethylgold(III) nitrate and dimethyl[tetrakis(pyrazol-1-yl)borato]gold(III).

Supplementary data available (No. SUP 56179, 8 pp.): thermal parameters, H-atom co-ordinates, least-squares planes. See Instructions for Authors, *J. Chem. Soc., Dalton Trans.*, 1985, Issue 1, pp. xvii—xix. Structure factors are available from the editorial office.

Table 1. Characterization data for the complexes

Complex	Analysis (%)[a]			Λ_M[b]	^{1}H N.m.r. at 15 °C[c]		
	C	H	N	Ω^{-1} cm^2 mol^{-1}	Me_2Au^{III}	*N*-Me	Other protons[d]
$[AuMe_2\{(mim)_2CHOH\}]NO_3$	27.3 (27.5)	3.8 (3.8)	14.7 (14.5)	91	1.23, **6**, *s*	3.90, **6**, *s*	6.21, **1**, *s*, C*H*OH; 7.26, **2**, *s* and 7.41, **2**, *s*, H(4) and H(5)
$[AuMe_2\{(mim)_3COH\}]NO_3$	32.0 (32.2)	3.9 (3.8)	17.8 (17.6)	88	0.93, **6**, *s*	4.09, **6**, *s*; 3.14, **3**, *s*	6.38, **1**, *d* [$J(H^4H^5)$ *ca.* 4 Hz], and 7.11, **3**, *br*, and 7.33, **2**, *br*, H(4) and H(5)
$[AuMe_2\{(py)(mim)_2COH\}]NO_3$	34.5 (34.4)	3.8 (3.8)	15.1 (15.1)	94	1.15, **6**, *s*[e]	3.93, **6**, *s*[e]	7.20—7.45, **5**, *m*, H(4) and H(5) (mim) and H(4) (py); 7.60—8.10, **2**, *m*, H(3) and H(5) (py); 8.51, **1**, *d*, H(6) [$J(H^5H^6)$ *ca.* 5 Hz][e]
$[AuMe_2\{(py)_2(mim)COH\}]NO_3$	36.5 (36.8)	3.5 (3.5)	12.8 (12.6)	94	0.85, **6**, *s*	3.23, **3**, *br*	7.08, **1**, *s* and 7.26, **1**, *s*, H(4) and H(5) (mim); 7.4—8.2, **6**, *m*, H(3,4,5) (py); 8.48, **2**, *br*, H(6)

[a] Calculated values are given in parentheses. [b] For *ca.* 10^{-3} mol dm^{-3} solutions in water. [c] Shifts are in p.p.m. from $SiMe_4$ for spectra of complexes in CD_3OD; given as chemical shift, **relative intensity**, *multiplicity*. [d] Assignment for H(4) and H(5) of *N*-methylimidazole rings not attempted. [e] At 45 °C owing to low solubility at 15 °C.

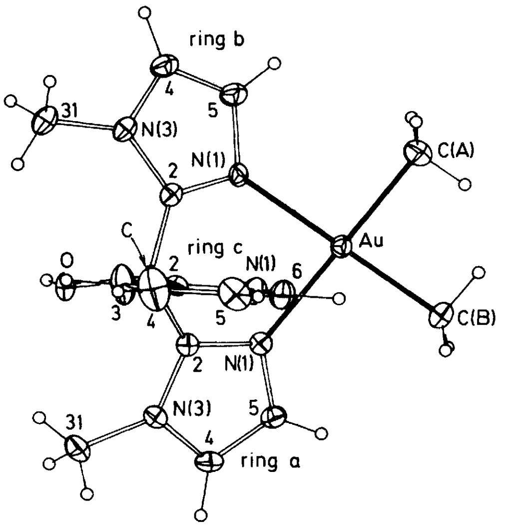

Figure 1. Structure of the cation $[AuMe_2\{(py)(mim)_2COH\}]^+$ projected onto the co-ordination plane and showing atom labelling

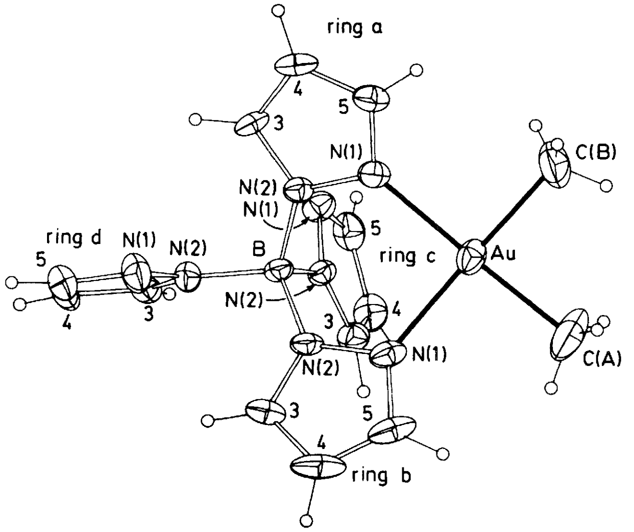

Figure 2. Structure of the complex $[AuMe_2\{B(pz)_4\}]$ projected onto the co-ordination plane and showing atom labelling

the complexes are given in Tables 2—6, and views of the complexes are shown in Figures 1 and 2.

The pyrazole, pyridine, and *N*-methylimidazole rings are planar [maximum deviation from mean plane is 0.053 Å for N(3) in ring b of the $(py)(mim)_2COH$ complex], and the nitrate ion is planar and regular (within 2σ in bond lengths and angles). The nitrate ion is not co-ordinated to gold in $[AuMe_2\{(py)(mim)_2COH\}]NO_3$, but is hydrogen bonded to the hydroxy-group of the ligand with O···O(1) 2.700(7) Å.

Both complexes have square-planar geometry for the gold atom, *cis*-C_2AuN_2 (Table 6), based on co-ordination of two *N*-methylimidazole groups in $[AuMe_2\{(py)(mim)_2COH\}]NO_3$ and two pyrazole groups in $[AuMe_2\{B(pz)_4\}]$, with the pyridine ring clearly unco-ordinated in the former [Au···N(c1) 3.317(6) Å with the gold atom −0.73(2) Å from the mean plane of the ring] and two pyrazole rings unco-ordinated in the latter (Figure 2). The complexes have Au···C and Au···N bond lengths within 1σ, and AuC_2 angles within 2σ, but with the AuN_2 angle somewhat smaller in the $(py)(mim)_2COH$ complex [85.2(2)°] than in the borate complex [89.6(3)°]. The complexes $[AuMe_2\{HB(pz)_3\}]$ (ref. 2) and $[AuMe_2\{B(pz)_4\}]$ have identical geometries (within 2σ in bond lengths and angles), and the complexes $[HgMeL]NO_3$ (ref. 6) and $[AuMe_2L]NO_3$ [L = $(py)(mim)_2COH$] have identical geometries for the organic ligand (within 2σ in bond lengths and angles) although the conformation and co-ordination mode of the ligands is different.

Proton N.M.R. Spectra for the Complexes $[AuMe_2L]NO_3$.—Proton n.m.r. spectra in CD_3OD exhibit relative intensities for Me_2Au^{III} and ligand protons consistent with the formulation $[AuMe_2L]NO_3$, and for the model bidentate ligand $(mim)_2CHOH$ the NMe and H(4,5) resonances are shifted downfield by 0.23 and 0.41, 0.46 p.p.m., respectively, on co-ordination (Table 1).

The complex $[AuMe_2\{(py)(mim)_2COH\}]NO_3$ appears to

Table 2. Non-hydrogen atom co-ordinates for $[AuMe_2\{(py)(mim)_2COH\}]NO_3$

Feature	Atom	*x*	*y*	*z*
Metal	Au	0.218 66(3)	0.538 33(3)	0.564 28(4)
Methyls	C(A)	0.182 4(10)	0.633 9(9)	0.790 0(12)
	C(B)	0.093 1(10)	0.650 3(9)	0.502 6(12)
$(py)(mim)_2COH$				
ring a	N(1)	0.246 1(6)	0.432 3(6)	0.337 7(7)
	C(2)	0.274 0(7)	0.313 2(7)	0.326 6(9)
	N(3)	0.257 8(6)	0.268 5(6)	0.175 6(8)
	C(31)	0.278 7(9)	0.144 4(8)	0.101 0(11)
	C(4)	0.220 4(8)	0.364 4(8)	0.087 8(10)
	C(5)	0.213 5(9)	0.463 5(8)	0.187 8(10)
ring b	N(1)	0.355 4(6)	0.426 6(5)	0.621 1(7)
	C(2)	0.380 7(7)	0.310 9(7)	0.568 3(9)
	N(3)	0.468 3(6)	0.266 8(6)	0.635 7(8)
	C(31)	0.524 7(10)	0.143 1(8)	0.621 3(12)
	C(4)	0.501 0(8)	0.359 2(8)	0.730 7(9)
	C(5)	0.431 5(8)	0.456 5(7)	0.721 3(10)
ring c	N(1)	0.128 6(6)	0.254 4(6)	0.697 8(8)
	C(2)	0.199 4(7)	0.176 3(6)	0.589 7(9)
	C(3)	0.175 0(9)	0.053 7(8)	0.584 0(13)
	C(4)	0.067 9(10)	0.010 1(9)	0.699 6(16)
	C(5)	−0.008 4(9)	0.088 6(8)	0.811 6(12)
	C(6)	0.025 4(8)	0.208 6(8)	0.805 6(10)
	C	0.313 4(7)	0.235 7(7)	0.462 8(9)
	O	0.389 2(5)	0.138 9(5)	0.378 6(6)
Nitrate	N	0.355 8(7)	0.819 3(7)	0.955 6(9)
	O(1)	0.444 0(6)	0.749 8(6)	0.888 5(8)
	O(2)	0.287 1(6)	0.794 4(7)	1.099 6(8)
	O(3)	0.336 6(8)	0.910 7(7)	0.871 1(10)

Table 3. Non-hydrogen atom co-ordinates for $[AuMe_2\{B(pz)_4\}]$

Feature	Atom	*x*	*y*	*z*
Metal	Au	0.345 35(3)	0.381 71(5)	0.340 56(2)
Methyls	C(A)	0.292 9(10)	0.194 5(19)	0.268 6(9)
	C(B)	0.428 9(10)	0.452 9(18)	0.255 5(7)
Boron	B	0.238(7)	0.589 6(9)	0.477 7(6)
Ring a	N(1)	0.404 3(5)	0.574 8(7)	0.412 2(4)
	N(2)	0.351 7(5)	0.643 4(6)	0.466 5(4)
	C(3)	0.409 1(6)	0.768 2(9)	0.499 4(5)
	C(4)	0.500 2(7)	0.780 1(10)	0.467 2(6)
	C(5)	0.495 4(7)	0.658 5(10)	0.414 2(6)
Ring b	N(1)	0.258 4(5)	0.303 6(8)	0.427 4(5)
	N(2)	0.233 5(5)	0.405 2(6)	0.485 2(4)
	C(3)	0.191 5(7)	0.319 4(11)	0.537 8(6)
	C(4)	0.188 8(9)	0.162 0(11)	0.515 4(9)
	C(5)	0.231 0(7)	0.155 4(10)	0.448 6(8)
Ring c	N(1)	0.159 3(5)	0.792 7(8)	0.380 6(4)
	N(2)	0.156 1(5)	0.640 9(6)	0.407 9(4)
	C(3)	0.067 0(6)	0.566 0(10)	0.374 8(5)
	C(4)	0.009 2(7)	0.670 9(12)	0.325 3(6)
	C(5)	0.070 8(8)	0.807 6(11)	0.330 6(5)
Ring d	N(1)	0.277 4(7)	0.635 0(10)	0.622 3(5)
	N(2)	0.211 8(6)	0.661 2(7)	0.552 0(4)
	C(3)	0.125 3(7)	0.749 8(9)	0.561 2(5)
	C(4)	0.134 3(9)	0.781 3(12)	0.639 6(6)
	C(5)	0.232 5(9)	0.707 5(13)	0.675 3(6)

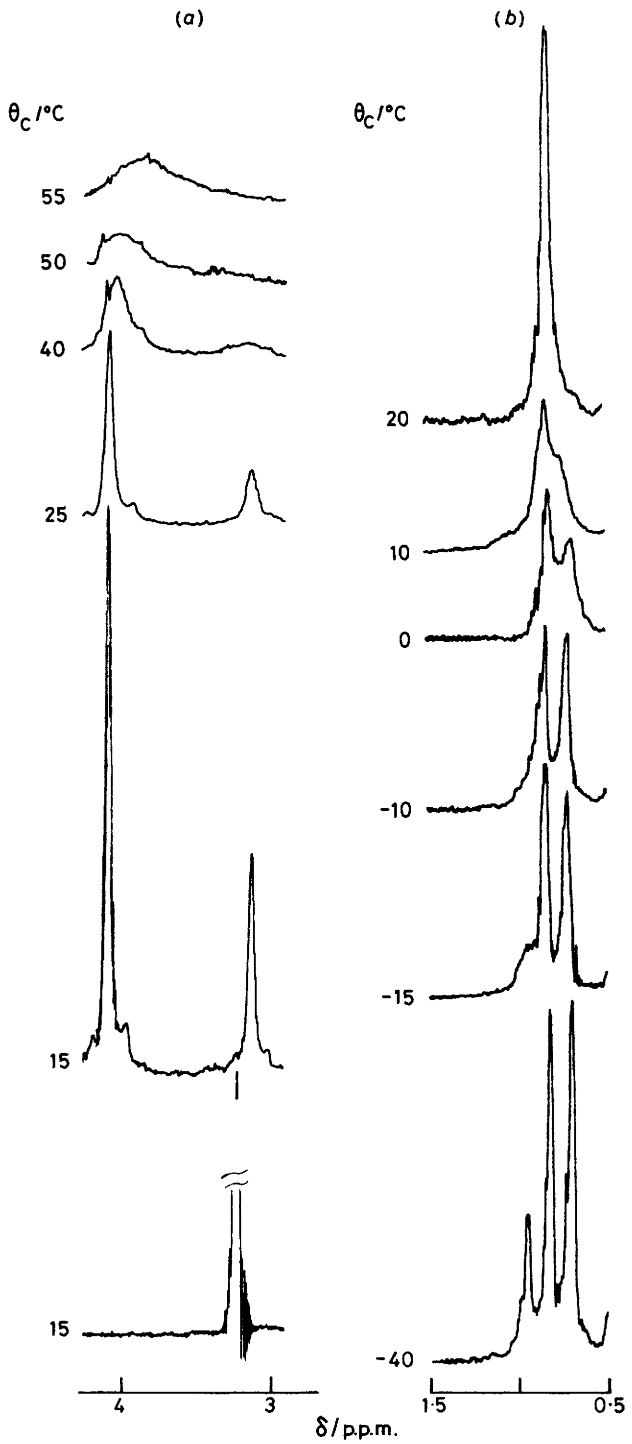

Figure 3. Examples of variable-temperature ^1H n.m.r. features for the cations $[AuMe_2L]NO_3$ in CD_3OD. (*a*) NMe resonances for $[AuMe_2\{(mim)_3COH\}]^+$ at 15—55 °C, and for $(mim)_3COH$ at 15 °C, (*b*) Me_2Au^{III} resonances for $[AuMe_2\{(py)_2(mim)COH\}]NO_3$ at −40 to 20 °C

have both imidazole groups as part of the *cis*-C_2AuN_2 group in methanol, as in the solid state (Figure 1). Thus, the NMe and H(4,5) resonances for the *N*-methylimidazole rings are shifted downfield by 0.51 and *ca.* 0.3—0.5 p.p.m., respectively, from the free-ligand values, while the pyridine resonances are virtually unaffected.

For the $(mim)_3COH$ complex, two imidazole environments in the ratio 2:1 are indicated at ambient temperature, with the predominant environment giving an NMe resonance (δ 4.09) shifted 0.73 p.p.m. downfield from that of the free ligand (δ 3.36), and the other environment giving an NMe resonance (δ 3.14) slightly upfield from that for the free ligand. Similarly, the ring protons H(4,5) exhibit resonances at δ 7.33, 7.11, and 6.38 in the ratio 2:3:1, compared with free-ligand values of δ 7.04 and 6.73,

Table 4. Geometry for $(py)(mim)_2COH$ and nitrate groups of $[AuMe_2\{(py)(mim)_2COH\}]NO_3$

$(py)(mim)_2COH$ rings

Atoms	Distance (Å) for ring mim (a)	 mim (b)	 py (c)
C–C(2)	1.52(1)	1.53(1)	1.54(1)
N(1)–C(2)	1.33(1)	1.34(1)	1.32(1)
N,C(3)–C(2)	1.36(1)	1.34(1)	1.36(1)
N(1)–C(5,6)	1.38(1)	1.37(1)	1.34(1)
C(4)–C(5)	1.34(1)	1.33(1)	1.37(1)
N,C(3)–C(4)	1.38(1)	1.38(1)	1.39(1)
N(3)–C(31)	1.47(1)	1.48(1)	—
C(5)–C(6)			1.36(1)

Atoms	Angle (°) for ring mim (a)	 mim (b)	 py (c)
C–C(2)–N(1)	126.3(7)	126.0(7)	114.3(6)
C–C(2)–N,C(3)	124.3(7)	124.7(6)	121.4(6)
N(1)–C(2)–N,C(3)	109.4(7)	109.1(7)	124.3(7)
C(2)–N(1)–C(5,6)	106.6(6)	107.4(7)	116.8(7)
N(1)–C(5)–C(4)	109.7(8)	108.5(7)	—
N,C(3)–C(4)–C(5)	106.6(6)	107.4(8)	120.4(9)
C(2)–N,C(3)–C(4)	107.7(6)	107.6(6)	117.0(8)
C(2)–N(3)–C(31)	130.6(7)	130.0(7)	—
C(4)–N(3)–C(31)	121.7(7)	122.4(8)	—
C(4)–C(5)–C(6)	—	—	117.4(8)
N(1)–C(6)–C(5)	—	—	124.2(8)
C(2)–N(1)–Au	125.4(5)	125.4(6)	—
C(5,6)–N(1)–Au	126.6(5)	127.1(5)	—

Apical carbon atom

Atoms	Distance (Å)
C–O	1.413(8)
	Angle (°)
O–C–C(a2)	109.4(5)
O–C–C(b2)	109.4(6)
O–C–C(c2)	107.2(5)
C(a2)–C–C(b2)	112.6(6)
C(a2)–C–C(c2)	109.0(6)
C(b2)–C–C(c2)	109.0(5)

Nitrate Atoms	Distance (Å)
N–O(1)	1.256(10)
N–O(2)	1.221(9)
N–O(3)	1.242(11)
O $\cdots$ O(1)*	2.700(7)
	Angle(°)
O(1)–N–O(2)	120.2(8)
O(1)–N–O(3)	119.2(7)
O(2)–N–O(3)	120.5(8)

* Transformation of the asymmetric unit (x, y, z,): $1 - x$, $1 - y$, $1 - z$.

Table 5. Geometry for the $[B(pz)_4]^-$ group in $[AuMe_2\{B(pz)_4\}]$

Atoms	Distance (Å) for ring a	 b	 c	 d
B–N(2)	1.54(1)	1.55(1)	1.52(1)	1.50(1)
N(1)–N(2)	1.36(1)	1.39(1)	1.35(1)	1.38(1)
N(2)–C(3)	1.34(1)	1.33(1)	1.34(1)	1.35(1)

Atoms	Distance (Å) for ring a	 b	 c	 d
N(1)–C(5)	1.34(1)	1.35(1)	1.31(1)	1.30(1)
C(4)–C(5)	1.36(1)	1.35(2)	1.38(1)	1.43(2)
C(3)–C(4)	1.36(1)	1.37(1)	1.35(1)	1.37(1)

Atoms	Angle (°) for ring a	 b	 c	 d
N(n2)–B–N(n + 1,2)	110.5(6)	108.4(6)	110.4(7)	109.2(6)
N(n2)–B–N(n + 2,2)	110.4(7)	107.8(7)	—	—
B–N(2)–N(1)	122.0(6)	122.1(7)	119.0(6)	120.5(7)
B–N(2)–C(3)	128.5(7)	128.1(8)	129.2(6)	127.9(7)
N(1)–N(2)–C(3)	109.2(6)	109.0(6)	110.9(6)	111.6(7)
N(2)–N(1)–C(5)	105.9(7)	105.4(8)	104.5(7)	106.2(8)

Atoms	Angle (°) for ring a	 b	 c	 d
N(1)–C(5)–C(4)	110.6(9)	110.5(9)	112.4(8)	109.9(9)
C(3)–C(4)–C(5)	105.7(8)	106.6(10)	104.5(8)	106.0(9)
C(4)–C(3)–N(2)	108.6(8)	108.5(10)	107.6(8)	106.3(8)
Au–N(1)–N(2)	124.4(5)	122.1(5)	—	—
Au–N(1)–C(5)	129.7(6)	131.7(7)	—	—

consistent with two ring environments in the ratio 2:1. The spectra thus indicate the presence of two strongly co-ordinated rings as part of the *cis*-C_2AuN_2 group, as for $[AuMe_2\{(py)(mim)_2COH\}]NO_3$, together with one other ring environment. At higher temperatures coalescence of NMe resonances occurs [Figure 3(*a*)], and the three resonances of H(3,4) coalesce to give two resonances, consistent with rapid equilibria between the strongly bound imidazole groups and the remaining ring. The remaining ring may be either weakly co-ordinated as in $[AuMe_2\{(pz)_3CH\}]NO_3$,[1] unco-ordinated but above the *cis*-C_2AuN_2 plane, as for the pyridine ring in $[AuMe_2\{(py)(mim)_2COH\}]NO_3$ (Figure 1) or $[AuMe_2\{(py)_3CH\}]NO_3$,[1] well removed from the gold atom as for ring d in $[AuMe_2\{B(pz)_4\}]$ (Figure 2), or in rapid equilibrium between some or all of these environments.

Proton n.m.r. spectra for $[AuMe_2\{(py)_2(mim)COH\}]NO_3$ exhibit complex variable-temperature behaviour. Two NMe environments are indicated at −40 °C with intensity ratio *ca.* 5:1 for resonances at δ 4.14 and 3.09, compared with 3.36 for the free ligand. These changes in chemical shift on complex formation are almost identical to those observed on complex formation by $(mim)_3COH$. The downfield resonance is assumed to arise from *N*-methylimidazole co-ordinated within the *cis*-C_2AuN_2 plane, with the lower-intensity resonance corresponding to a different *N*-methylimidazole environment, and thus the spectra indicate the presence of co-ordination

Table 6. Co-ordination geometry for the gold atom in the complexes[a]

	Distance			Angles			Deviation[b]	
Atoms	(py)(mim)$_2$COH complex	[B(pz)$_4$]$^-$ complex	Atoms	(py)(mim)$_2$COH complex	[B(pz)$_4$]$^-$ complex	Atoms	(py)(mim)$_2$COH complex[c]	[B(pz)$_4$]$^-$ complex[d]
Au–C(A)	2.024(9)	2.04(2)	C(A)–Au–C(B)	85.0(4)	86.4(6)	Au	0.009	−0.010
Au–C(B)	2.030(11)	2.03(1)	C(A)–Au–N(a1)	176.3(3)	177.8(6)	C(A)	−0.084	0.005
Au–N(a1)	2.098(6)	2.096(6)	C(A)–Au–N(b1)	95.5(5)	92.5(5)	C(B)	0.080	−0.005
Au–N(b1)	2.113(7)	2.101(8)	C(B)–Au–N(a1)	94.4(3)	91.6(4)	N(a1)	−0.029	0.005
			C(B)–Au–N(b1)	177.5(3)	178.8(6)	N(b1)	0.028	−0.005
			N(a1)–Au–N(b1)	85.2(2)	89.6(3)			

[a] Distances and deviations in Å; angles in °. [b] Deviation from the AuC$_2$N$_2$ planes, where the right-hand orthogonal Å frame (X, Y, Z) has X parallel to a, Z in the ac plane. [c] $0.5974X + 0.6447Y - 0.2879Z = 3.959$, $\chi^2 = 87.9$. [d] $0.7241X - 0.5515Y + 0.4141Z = 3.148$, $\chi^2 = 0.8$.

geometries '*cis*-Me$_2$Au(py)(mim)' and '*cis*-Me$_2$Au(py)$_2$' in *ca.* 5:1 ratio. Consistent with this interpretation, the Me$_2$Au^{III} group gives three resonances at δ 0.96, 0.83, and 0.71 in the ratio *ca.* 2:5:5 at −40 °C [Figure 3(*b*)], for methyl groups *trans* to py in '*cis*-Me$_2$Au(py)$_2$,' *trans* to py in '*cis*-Me$_2$Au(py)(mim),' and *trans* to mim in '*cis*-Me$_2$Au(py)(mim),' respectively. At higher temperatures the Me$_2$Au^{III} resonances coalesce to a single resonance at δ 0.85 (20 °C) (expected value *ca.* 0.80 for coalescence of resonances in ratio *ca.* 2:5:5 at −40 °C), the NMe resonances broaden and then give rise to a single resonance at δ 4.03 (expected value *ca.* 3.96), and simplify to allow partial assignment (Table 1). Thus, the variable-temperature spectra indicate the presence of rapid equilibria between the two structural isomers.

*Proton N.M.R. Spectra for Protonated Poly(pyrazol-*1*-yl)borate Complexes.*—The complexes [AuMe$_2${HB(pz)$_3$}] and [AuMe$_2${B(pz)$_4$}] exhibit complex variable-temperature ^{1}H n.m.r. spectra in CD$_2$Cl$_2$,[2] with the former showing resonances for co-ordinated and free pyrazole rings at −90 °C, and the latter showing co-ordinated pyrazole together with two inequivalent unco-ordinated pyrazole environments at −90 °C (as in Figure 2).

The complexes are insoluble in water but dissolve on addition of dilute HCl. For the complexes in dioxane–water (1:1), potentiometric studies involving treatment of titration data with the programs MINIQUAD 75 (ref. 7) and MINIQUAD 81 (ref. 8) allowed determination of protonation constants as in equations (1) and (2).

$$[\mathrm{AuMe_2\{HB(pz)_2(Hpz)\}}]^+ \rightleftharpoons [\mathrm{AuMe_2\{HB(pz)_3\}}] + \mathrm{H^+};\ \mathrm{p}K = 3.69(2) \quad (1)$$

$$[\mathrm{AuMe_2\{B(pz)_3(Hpz)\}}]^+ \rightleftharpoons [\mathrm{AuMe_2\{B(pz)_4\}}] + \mathrm{H^+};\ \mathrm{p}K = 1.91(2) \quad (2)$$

Proton n.m.r. spectra of the cations were obtained using (CD$_3$)$_2$SO–D$_2$O (1:1) solutions to which CF$_3$CO$_2$D was added, for comparison with spectra of the cations [AuMe$_2$L]$^+$ discussed above. Spectra are shown in Figure 4, together with those of protonated K[HB(pz)$_3$] and K[B(pz)$_4$] obtained under the same conditions to assist with interpretation. The assignment of H(4) resonances is given; assignments for H(3) and H(5) are not attempted, as usual for poly(pyrazol-1-yl)borate complexes.[9]

Spectra of the protonated complexes (Figure 4) differ from those of the neutral complexes,[2] with resonances shifted downfield by 0.3—0.7 p.p.m. on protonation and change of solvent. For [AuMe$_2${HB(pz)$_2$(Hpz)}]$^+$, the presence of both co-ordinated and protonated pyrazole environments is clearly

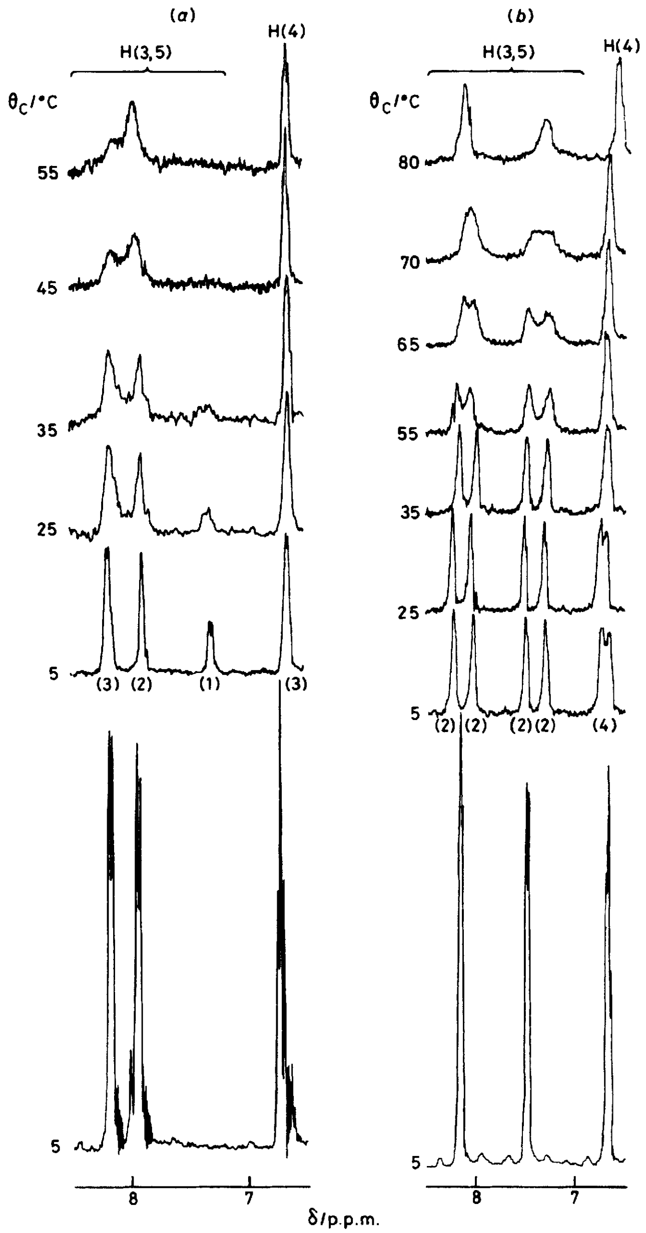

Figure 4. Variable-temperature ^{1}H n.m.r. spectra of (*a*) [AuMe$_2${HB(pz)$_2$(Hpz)}]$^+$ and (*b*) [AuMe$_2${B(pz)$_3$(Hpz)}]$^+$ in (CD$_3$)$_2$SO–D$_2$O–CF$_3$CO$_2$D. Relative intensities are given in parentheses, and spectra of protonated K[HB(pz)$_3$] and K[B(pz)$_4$] under the same conditions are given for 5 °C only

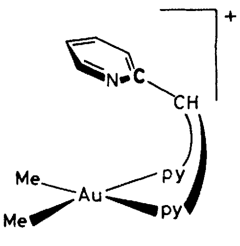

(1)

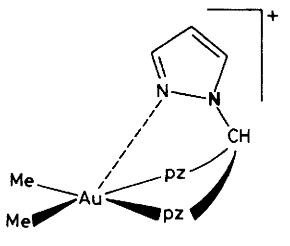

(2)

illustrated at 5 °C, as there are four resonances with relative intensities 3:2:1:3, *i.e.* 2 H + 1 H:2 H:1 H:2 H + 1 H for pyrazole environments in the ratio 2:1 (co-ordinated:protonated). Similarly, for $[AuMe_2\{B(pz)_3(Hpz)\}]^+$, six proton environments are indicated at 5 °C, corresponding to two (equivalent) co-ordinated rings and two unco-ordinated rings. Environments for the unco-ordinated rings (protonated, deprotonated, and ring positions similar to those of c and d in Figure 2) are expected to be exchanging rapidly *via* protonation–deprotonation equilibria and conformational changes of the Au–N–N–B–N–N six-membered ring.

Discussion

For the five complexes studied by *X*-ray diffraction, only the $(pz)_3CH$ complex involves a weak axial interaction, in addition to the regular square-planar co-ordination *cis*-C_2AuN_2 present in all of the complexes.

The Lewis acidity of the *cis*-C_2AuN_2 kernel is clearly very low, and it has been proposed that the ligand geometry of bidentate $(pz)_3CH$ allows rotation of the axial pyrazole group, about the N–C(H) bond in **(2)** to give a long Au···N interaction consistent with the low acidity of the gold atom.[1] Bidentate $(py)_3CH$ has Au···C 3.064(12) Å, as in **(1)**, much shorter than the corresponding distance Au···N, 3.703(5) Å, for the $(pz)_3CH$ complex **(2)**, and thus rotation of the axial pyridine ring about C–C(H) results in an axial Au···N distance similar to that for the pyridine groups that are strongly bound within the square plane, and thus inappropriate for the low acidity of gold.

The poly(pyrazol-1-yl)borate complexes and $[AuMe_2\{(py)(mim)_2COH\}]NO_3$ are expected to have similar Au···N (borates) and Au···C $(py)(mim)_2COH$ distances to Au···N for the $(pz)_3CH$ complex, since they have five-membered rings co-ordinated in the square plane. Thus, $[AuMe_2\{B(pz)_4\}]$ has Au···N 3.556(6) and $[AuMe_2\{(py)(mim)_2COH\}]NO_3$ has Au···C 3.937(7) Å, resulting in potential Au···N (axial) distances similar to that for the $(pz)_3CH$ complex. In contrast to the $(pz)_3CH$ complex these complexes do not involve a weak axial interaction, perhaps as a result of the higher basicity of borate and imidazole-based ligands further lowering the Lewis acidity of the gold centre on co-ordination of the ligands as bidentates, *e.g.* $[B(pz)_4]^-$ has pK_1 7.10, $(mim)_3COH$ has pK_1 5.25,[4] but $(pz)_3CH$ has $pK_1 < ca.$ 1.2 in dioxane–water (1:1).[5]

A similar effect of increasing basicity has been observed for $MeHg^{II}$ with the tripod ligands $(py)_n(mim)_{3-n}COH$ (n = 0—3) in complexes $[HgMeL]NO_3$, where the $MeHg^{II}$ moiety forms one strong Hg–N bond with additional weaker interaction(s),[3,4,6] *e.g.* $(py)_3COH$ is present as a tridentate with Hg–N 2.28(1), 2.45(1), and 2.53(1) Å, but the more basic $(mim)_3COH$ is present as a bidentate involving one Hg–N bond of 2.125(7) Å and a weak Hg···OH interaction of 2.680(6) Å (ref. 4).

The Me_2Au^{III} cation binds to the more basic *N*-methylimidazole groups of the tripod ligand $(py)(mim)_2COH$ in both the solid state and solution, and for $(py)_2(mim)COH$ the isomer involving *N*-methylimidazole binding predominates in solution. Similarly, $MeHg^{II}$ binds more strongly to the *N*-methylimidazole groups in its complexes with these ligands.[3,4,6]

Although weak axial interaction is clearly demonstrated only for $[AuMe_2\{(pz)_3CH\}]NO_3$, the complexes $[AuMe_2\{HB(pz)_3\}]$ and $[AuMe_2\{B(pz)_4\}]$,[2] $[AuMe_2L]NO_3$ [L = $(mim)_3COH$ or $(py)_2(mim)COH$], $[AuMe_2\{HB(pz)_2(Hpz)\}]^+$, and $[AuMe_2\{B(pz)_3(Hpz)\}]^+$ in solution exhibit variable-temperature ^1H n.m.r. spectra indicating rapid exchange between co-ordinated and unco-ordinated donor groups, consistent with the facile formation of intermediates with geometry perhaps closely related to that of $[AuMe_2\{(pz)_3CH\}]NO_3$. For the complex $[AuMe_2\{HB(pz)_2(Hpz)\}]^+$, exchange in this manner requires deprotonation of the unco-ordinated ring. An intramolecular mechanism, involving five-co-ordinate intermediates, is similar to that envisaged for intermolecular exchange of pyridine by $AuMe_2Cl(C_5H_5N)$ in pyridine,[10] and is typical for unidentate ligand-substitution reactions for square-planar complexes.

Experimental

Preparation and Characterization of Complexes.—The neutral ligands were synthesized as reported,[11,12] and the poly(pyrazol-1-yl)borate salts were used as received (Columbia Organic Chemicals Company, Inc.); dimethylgold(III) iodide was prepared from $AuCl_3(C_5H_5N)$,[13] which was obtained from laboratory residues of gold as described.[1] The Me_2Au^{III} complexes were obtained in moderate yield (34—77%) by a similar procedure to that described for other complexes $[AuMe_2L]NO_3$ involving reaction of equimolar quantities of dimethylgold(III) nitrate and ligand in water,[1] followed by slow evaporation at ambient temperature, collection of the product by filtration, and recrystallization from methanol–water (1:1) [L = $(mim)_2CHOH$, $(mim)_3COH$, $(py)(mim)_2COH$] or chloroform–ethyl acetate (1:1) [L = $(py)_2(mim)COH$]. The complexes $[AuMe_2\{HB(pz)_3\}]$ and $[AuMe_2\{B(pz)_4\}]$ were prepared as reported,[2] and protonation constants for these complexes, and for $K[B(pz)_4]$ in dioxane–water (1:1), were measured as described elsewhere.[14–16] Proton n.m.r. spectra were recorded with a JEOL JNM-4H-100 spectrometer. Conductivities were measured with a Philips PW 9504/00 conductivity meter in water, and microanalyses were by the Australian Microanalytical Service.

Crystallography.—Crystals of $[AuMe_2\{(py)(mim)_2COH\}]NO_3$ were obtained from methanol–water (1:1), and crystals of $[AuMe_2\{B(pz)_4\}]$ were obtained by dissolution of the complex in dilute HCl and slow neutralization of this by vapour transport of pyridine, as described earlier.[2]

For each complex a unique data set was measured at 295 K to $2\theta_{max.}$ 50° using Syntex $P\bar{1}$ [$(py)(mim)_2COH$ complex] and $P2_1$ {$[B(pz)_4]^-$ complex} four-circle diffractometers in conventional 2θ—θ scan mode with Mo-K_α radiation (λ 0.71069 Å), yielding N independent reflections; N_o of these with $I > 3\sigma(I)$ were considered 'observed' and used in the structure solution and refinement after the application of analytical absorption corrections and with statistical weights. Full-matrix least-squares [$(py)(mim)_2COH$ complex] and 9 × 9 block-diagonal least-squares {$[B(pz)_4]^-$ complex} refinements were employed, with anisotropic thermal parameters refined for the non-hydrogen atoms, and hydrogen atoms included at calculated positions (x, y, z, U) and constrained. Neutral atom scattering factors were used, those for the non-hydrogen atoms being corrected for anomalous dispersion (f', f'').[17] Computation used the XTAL 83 [$(py)(mim)_2COH$ complex] and *X*-RAY 76[18] {$[B(pz)_4]^-$ complex} program systems implemented by Dr. S. R. Hall on a Perkin-Elmer 3240 computer.

Crystal data.—$[AuMe_2\{(py)(mim)_2COH\}]NO_3$, $C_{16}H_{21}$-AuN_6O_4, $M = 558.4$, triclinic, space group $P\bar{1}$ (C^1_i, no. 2), $a = 11.393(3)$, $b = 10.859(2)$, $c = 7.927(2)$ Å, $\alpha = 89.16(2)$, $\beta = 74.11(2)$, $\gamma = 89.87(2)^\circ$, $U = 943.1(4)$ Å^3, $D_c(Z = 2) = 1.97$ g cm^{-3}, $F(000) = 540$. Specimen size 0.28 × 0.04 × 0.21 mm, $\mu = 76$ cm^{-1}; $N = 3\,218$, $N_o = 2\,801$, $R = 0.034$, $R' = 0.038$.

$[AuMe_2\{B(pz)_4\}]$, $C_{14}H_{18}AuBN_8$, $M = 506.1$, monoclinic, space group $P2_1/c$ (C^5_{2h}, no. 14), $a = 12.645(2)$, $b = 8.343(2)$, $c = 17.310(4)$ Å, $\beta = 99.14(2)^\circ$, $U = 1\,802.8(7)$ Å^3, $D_m = 1.87(1)$, $D_c\,(Z = 4) = 1.87$ g cm^{-3}, $F(000) = 968$. Specimen size 0.36 × 0.28 × 0.08 mm, $\mu = 93$ cm^{-1}; $N = 3\,186$, $N_o = 2\,240$, $R = 0.040$, $R' = 0.044$.

Acknowledgements

This work was supported by the Australian Research Grants Scheme.

References

1 A. J. Canty, N. J. Minchin, P. C. Healy, and A. H. White, *J. Chem. Soc., Dalton Trans.*, 1982, 1795.

2 A. J. Canty, N. J. Minchin, J. M. Patrick, and A. H. White, *Aust. J. Chem.*, 1983, **36**, 1107.

3 A. J. Canty, N. Chaichit, B. M. Gatehouse, and E. E. George, *Inorg. Chem.*, 1981, **20**, 4293.

4 A. J. Canty, J. M. Patrick, and A. H. White, *J. Chem. Soc., Dalton Trans.*, 1983, 1873.

5 A. J. Canty and C. V. Lee, unpublished work.

6 A. J. Canty, J. M. Patrick, and A. H. White, *Inorg. Chem.*, 1984, **23**, 3827.

7 P. Gans, A. Sabatini, and A. Vacca, *Inorg. Chim. Acta*, 1976, **18**, 237.

8 R. N. Sylva and M. R. Davidson, *J. Chem. Soc., Dalton Trans.*, 1979, 465.

9 See, for example, S. Trofimenko, *J. Am. Chem. Soc.*, 1967, **89**, 3170.

10 H. Hagnauer, G. C. Stocco, and R. S. Tobias, *J. Organomet. Chem.*, 1972, **46**, 179.

11 R. S. Brown and J. Huguet, *Can. J. Chem.*, 1980, **58**, 889.

12 A. J. Canty, E. E. George, and C. V. Lee, *Aust. J. Chem.*, 1983, **36**, 415.

13 F. H. Brain and C. S. Gibson, *J. Chem. Soc.*, 1931, 762.

14 A. J. Canty and A. Marker, *Inorg. Chem.*, 1976, **15**, 425.

15 A. J. Canty, N. Chaichit, B. M. Gatehouse, E. E. George, and G. Hayhurst, *Inorg. Chem.*, 1981, **20**, 2414.

16 A. J. Canty and C. V. Lee, *Organometallics*, 1982, **1**, 1063.

17 J. A. Ibers and W. C. Hamilton (eds.), 'International Tables for *X*-Ray Crystallography,' Kynoch Press, Birmingham, 1974, vol. 4.

18 The *X*-RAY System and the XTAL System, Technical Reports, TR-446 and TR-1364, Computer Science Center, University of Maryland, 1976 and 1983.

Received 23*rd July* 1984; *Paper* 4/1279